

DiffSketcher: Text Guided Vector Sketch Synthesis through Latent Diffusion Models

Ximing Xing
Beihang University
ximingxing@buaa.edu.cn

Chuang Wang
Beihang University
18377011@buaa.edu.cn

Haitao Zhou
Beihang University
18377221@buaa.edu.cn

Jing Zhang
Beihang University
zhang_jing@buaa.edu.cn

Qian Yu*
Beihang University
qianyu@buaa.edu.cn

Dong Xu
HongKong University
dongxu@cs.hku.hk

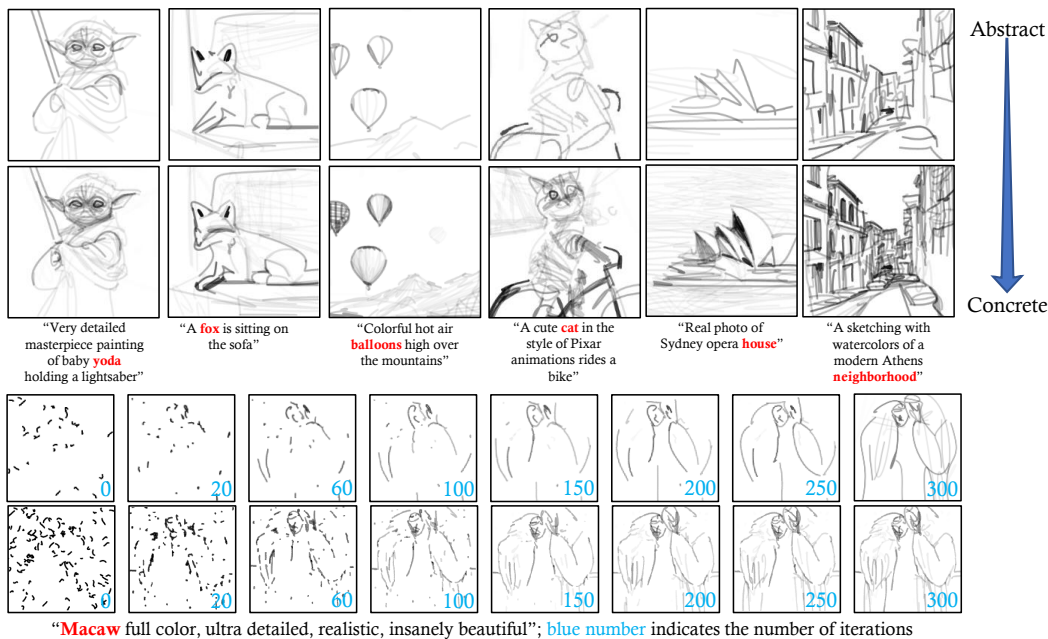


Figure 1: **Top:** Visualizations of the vector sketches generated by our proposed method, *DiffSketcher*. **Bottom:** Visualizations of the drawing process. For each example, we show two sketches with a different number of strokes.

Abstract

Even though trained mainly on images, we discover that pretrained diffusion models show impressive power in guiding sketch synthesis. In this paper, we present DiffSketcher, an innovative algorithm that creates *vectorized* free-hand sketches using natural language input. DiffSketcher is developed based on a pre-trained text-to-image diffusion model. It performs the task by directly optimizing a set of Bézier curves with an extended version of the score distillation sampling (SDS) loss, which allows us to use a raster-level diffusion model as a prior for optimizing a parametric vectorized sketch generator. Furthermore, we explore attention maps

*Corresponding author

embedded in the diffusion model for effective stroke initialization to speed up the generation process. The generated sketches demonstrate multiple levels of abstraction while maintaining recognizability, underlying structure, and essential visual details of the subject drawn. Our experiments show that DiffSketcher achieves greater quality than prior work. The code and demo of DiffSketcher can be found at <https://ximinng.github.io/DiffSketcher-project/>.

1 Introduction

Minimal representations, such as sketches and natural language, are powerful tools for effectively conveying ideas by emphasizing the subject’s essence. As the carriers of abstract concepts, natural language conveys abstract semantic understanding, whereas sketches embody the human visual abstract presentation. A sketch can provide more visual details than natural language, making the concept more concrete. When a designer discusses the design plan with a client, the designer may sketch a prototype based on the client’s description to ensure a full understanding of his/her requirements. If the process of text-to-sketch could be learned automatically, it would significantly lessen associated labor costs.

Unfortunately, the task of text-to-sketch remains unexplored. Some studies have been conducted on generating image-conditioned sketches [3, 18, 44, 43]. One such method is Info-drawing [3], which treats a sketch as a photo and uses a generative adversarial network (GAN) to generate a raster sketch based on an input image. It also introduces a style loss to ensure the generated sketches have a similar style to the reference sketch used in training. CLIPasso [44] presents a novel pipeline to produce vector sketches through a differentiable rasterizer optimized by a semantic loss. CLIPasso can only handle the images with a single object, so its follow-up work CLIPascene [43] extends to scene-level images. However, all of these methods depend on input images and do not facilitate the generation of sketches directly from text inputs. Moreover, despite their ability to generate realistic sketches from photos, these methods have a limitation in that they cannot generate *new content*.

Recent breakthroughs in text-to-image generation have been driven by diffusion models [23, 28, 30, 31] trained on billions of image-text pairs [34]. These models, conditioned on text, now support high-fidelity, diverse, and controllable image synthesis. Nonetheless, the present text-to-image diffusion models cannot produce highly abstract and vectorized free-hand sketches (as shown in Fig. 2). We draw inspiration from the highly effective text-to-image diffusion models and image-conditioned sketch generators to build a bridge between two fundamental forms of human expression, namely text and free-hand sketches, resulting in the development of our proposed text-to-sketch generator.

In this work, we present DiffSketcher, an algorithm that can synthesize novel and high-quality free-hand vector sketches based on natural language text input. DiffSketcher does not require any text-to-sketch training pairs or large datasets of sketches. Instead, with the guidance of a pretrained diffusion model [30], we define a sketch as a set of Bézier curves and optimize the curves’ parameters through a differentiable rasterizer [16]. The key idea behind DiffSketcher is to transfer the prior knowledge from text-to-image generation model into the differentiable rasterizer. This allows the optimization of text-guided sketches with semantic consistency, ensuring that the final output sketches are coherent and aligned with their corresponding text inputs. However, it is a non-trivial task to fully leverage the pre-trained diffusion model to efficiently generate high-quality free-hand sketches for both simple objects and complex scenes.

To this end, we propose three strategies to improve the generation quality and efficiency: (1) Present an extended Score Distillation Sampling (SDS) Loss to guide the optimization of curve parameters. Previous works optimize the parameters of the vector sketch with CLIP loss. We found that an extended version of SDS loss can give more diverse sketch synthesis results, and it can be combined with CLIP loss or LPIPS loss, providing an additional control term. (2) Explore attention maps embedded in the diffusion model for effective stroke initialization. The synthesis process can be very time-consuming if the starting point of each stroke is randomly initialized. Therefore, we explore different initialization strategies and present to initialize the curve control points with a fused product of cross-attention maps and self-attention maps in the U-Net [5] of the diffusion model, which significantly improves the efficiency compared to the random initialization. (3) Introduce opacity property during the optimization of Bézier curves to better mimic the style of human sketches, achieving the effect of heavy and light brushstrokes.

Our contributions are threefold: (1) We propose a text-to-sketch diffusion model dubbed DiffSketcher. To the best of our knowledge, it is the first diffusion model to generate diverse and high-quality vector sketches with different levels of abstraction at the object and scene levels. (2) We present three strategies to improve the generation quality and efficiency, including an extended SDS loss and an attention-enhanced stroke initialization strategy. The opacity property of strokes is considered during synthesis to improve the visual effect further. (3) We conduct extensive experiments, and the experimental results show that our model outperforms other models in sketch quality and diversity. Thorough insights are provided for future research.

2 Related Work

Sketch Synthesis. Free-hand drawings convey abstract concepts through human visual perception with minimal abstraction. Unlike purely edge-map extraction methods [2], free-hand sketching aims to present sketches that are abstract in terms of structure [3] and semantic interpretation[44]. Therefore, computational sketching methods that aim to mimic human drawing consider a wide range of sketch representations, ranging from those grounded in the edge map of the input image[45, 17, 15, 41, 18, 4] to those that are more abstract [9, 8, 1, 7, 26, 44], which are normally in vector format. Among the works synthesizing vector sketches, CLIPasso [44] and Clipascene [43] are conditioned on an input image, while the rest are unconditional. Until now, no prior work has explored synthesizing a sketch based on text.

Vector Graphics. Our work builds upon the differentiable renderer for vector graphics introduced by Li et al [16]. While image generation methods that operate over vector images traditionally require a vector-based dataset, recent work has shown how differentiable renderers can be used to bypass this limitation [36, 14, 40, 29, 19]. Furthermore, recent advances in visual text embedding contrastive language-image pre-training (CLIP)[27] have enabled a number of successful methods for synthesizing sketches, such as CLIPDraw[7], StyleCLIPDraw [32], CLIP-CLOP [21], and CliPascene [43]. A very recent work VectorFusion [13] combine differentiable renderer with diffusion model for vector graphics generation, *e.g.*, iconography and pixel art. Our proposed algorithm, DiffSketcher, shares a similar idea with VectorFusion, but our focus is generating object- and scene-level sketches from a natural language prompt.

Diffusion Models. Denoising diffusion probabilistic models (DDPMs) [37, 38, 11, 39], particularly those conditioned on text, have shown promising results in text-to-image synthesis. For example, Classifier-Free Guidance (CFG)[12] has improved sample quality and has been widely used in large-scale diffusion model frameworks, including GLIDE[23], Stable Diffusion [30], DALL·E 2 [28], and Imagen [31]. However, the majority of images available in web-scale datasets are rasterized, and this work follows the framework of *synthesis through optimization*, in which images are generated through evaluation-time optimization against a given metric. Our proposed algorithm, *DiffSketcher*, uses a pre-trained text-to-image diffusion model to synthesize free-hand sketches from natural language input. This is achieved by transferring image synthesis prior information into a differentiable renderer.

3 Preliminaries

3.1 Diffusion Models

In this section, we provide a concise overview of diffusion models, which are a class of generative models that utilize latent variables to gradually transform a sample from a noise distribution to a target data distribution [37, 11]. Diffusion models consist of two components: a forward process q and a reverse process or generative model p . The forward process, which is typically modeled as a Gaussian distribution, gradually removes structure from the input data x by adding noise over time. The reverse process, on the other hand, adds structure to the noise starting from a latent variable \mathbf{z}_t . Specifically, the generative model is trained to slowly add structure starting from random noise $p(\mathbf{z}_T) = \mathcal{N}(\mathbf{0}, \mathbf{I})$ with transitions $p_\phi(\mathbf{z}_{t-1}|\mathbf{z}_t)$. $q(\mathbf{z}_t|\mathbf{x}) = \mathcal{N}(\alpha_t\mathbf{x}, \sigma_t^2\mathbf{I})$. Training the diffusion model with a (weighted) evidence lower bound (ELBO) simplifies to a weighted denoising score matching objective for parameters ϕ [11]

$$\mathcal{L}_{\text{Diff}}(\phi, \mathbf{x}) = \mathbb{E}_{t \sim \mathcal{U}(0,1), \epsilon \sim \mathcal{N}(\mathbf{0}, \mathbf{I})} \left[w(t) \|\epsilon_\phi(\alpha_t\mathbf{x} + \sigma_t\epsilon; t) - \epsilon\|_2^2 \right] \quad (1)$$

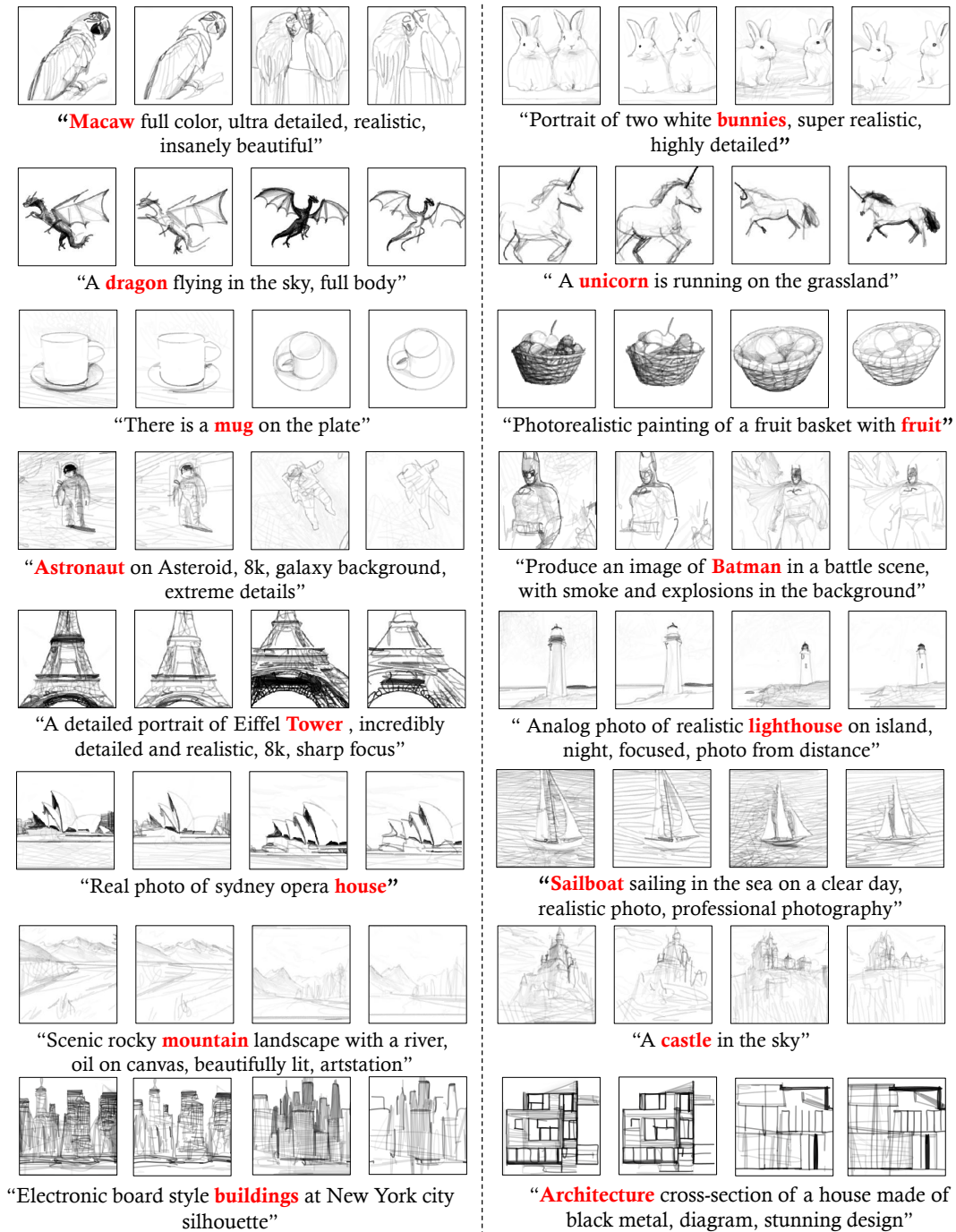


Figure 2: Various free-hand sketches synthesized by DiffSketcher and the corresponding description prompts. DiffSketcher obtains prior information from LDM [30] composite images through score distillation [24] and achieves the same heavy and light drawing styles as human sketches by performing gradient descent on a set of Bézier curves with the opacity property. Our proposed DiffSketcher allows for varying levels of abstraction while matching its corresponding textual semantics. In each example, given the same text prompt and two different random seeds, two sketches with a different number of strokes are generated. The red words represent the cross-attention index used to initialize the control points (details about cross-attention are covered in Section 4.2).

where $w(t)$ is a weighting function that depends on the timestep t . Our work builds on text-to-image latent diffusion model (LDM) that learn $\epsilon_\phi(\mathbf{z}_t; t, y)$ conditioned on text embeddings y [30]. LDM uses classifier-free guidance(CFG) [12], which jointly learns an unconditional model to enable higher quality generation via a guidance scale parameter ω : $\hat{\epsilon}_\phi(\mathbf{z}_t; y, t) = (1 + \omega)\epsilon_\phi(\mathbf{z}_t; y, t) - \omega\epsilon_\phi(\mathbf{z}_t; t)$ ($\hat{\epsilon}_\phi$ denotes the guided version of the noise prediction). CFG alters the score function to prefer regions where the ratio of the conditional density to the unconditional density is large. In practice, setting $w > 0$ improves sample fidelity at the cost of diversity.

3.2 Score Distillation Sampling

Many 3D generative approaches use a frozen image-text joint embedding model (e.g. CLIP) and an optimization-based approach to train a Neural Radiance Fields (NeRF) [20]. Such models can be specified as a differentiable image parameterization (DIP) [22], where a differentiable generator g transforms parameters θ to create an image $\mathbf{x} = g(\theta)$. In DreamFusion [24], θ be parameters of a 3D volume and g is a volumetric renderer. To learn these parameters, DreamFusion proposed *score distillation sampling* (SDS) loss that can be applied to Imagen [31]:

$$\nabla_\theta \mathcal{L}_{\text{SDS}}(\phi, \mathbf{x} = g(\theta)) \triangleq \mathbb{E}_{t, \epsilon} \left[\omega(t) (\hat{\epsilon}_\phi(\mathbf{z}; y, t) - \epsilon) \frac{\partial \mathbf{x}}{\partial \theta} \right] \quad (2)$$

where the constant $\alpha_t \mathbf{I} = \partial \mathbf{z}_t / \partial \mathbf{x}$ absorbed into $w(t)$, and use the classifier-free-guided $\hat{\epsilon}_\phi$. In practice, SDS gives access to loss gradients, not a scalar loss. Their proposed SDS loss provides a way to assess the similarity between an image and a caption:

$$\nabla_\theta \mathcal{L}_{\text{SDS}}(\phi, \mathbf{x} = g(\theta)) = \nabla_\theta \mathbb{E}_t [\sigma_t / \alpha_t w(t) \text{KL}(q(\mathbf{z}_t | g(\theta); y, t) | p_\phi(\mathbf{z}_t; y, t))] \quad (3)$$

where p_ϕ is the distribution learned by the frozen, pretrained Imagen model. q is a unimodal Gaussian distribution centered at a learned mean image $g(\theta)$. DreamFusion [24] proposed an approach to use a pretrained pixel-space text-to-image diffusion model (Imagen [31]) as a loss function. However, diffusion models trained on pixels have traditionally been used to sample only pixels. We want to create what look like good sketches that match the text prompts when rendered from a set of vector strokes. Such models can be specified as a differentiable image parameterization, where a differentiable rasterizer \mathcal{R} transforms parameters θ to create a sketch $\mathcal{S} = \mathcal{R}(\theta)$.

Inspired by DreamFusion [24], we extend *score distillation sampling* (SDS) loss to use a pretrained latent diffusion model [30] as a prior for optimizing curve parameters. Intuitively, score distillation converts diffusion sampling into an optimization problem that allows the raster image to be represented by a differentiable rasterizer.

3.3 Differentiable Rasterizer

Li *et al.* [16] introduce a differentiable rasterizer \mathcal{R} that bridges the vector graphics and raster image domains. A raster image is a 2D grid sampling over the space of the vector graphics scene $f(x, y; \Theta)$, where Θ contains the curve parameters, e.g., coordinates of Bézier control points, opacity, line thickness. Given a 2D location $(x, y) \in \mathbb{R}^2$, they first find all the filled curves and strokes that overlap with the location. Then sort them with a user-specified order and compute the color using alpha blending [25]. It enables the gradients of the rasterized curves (image) to be backpropagated to the curve parameters.

4 Methodology

In this section, we present our method for generating sketches using pre-trained text-to-image diffusion models. Let \mathcal{S} be a sketch that was rendered by a differentiable rendering [16] \mathcal{R} using the text prompt \mathcal{P} . Our goal is to optimize a set of parametric strokes to automatically generate a vector sketch that matches the description of the text prompt.

Our pipeline is illustrated in Figure 3. Given a text prompt y of the desired subject and a set of control points, we synthesize the corresponding sketch \mathcal{S} while matching the semantic attributes of the text prompt. To initialize the locations of the strokes, we extract and fuse the attention map of the U-Net [5] used by the latent diffusion model [30]. Our key observation is that the structure and appearance of the generated image depend on the interaction between the pixels and the text embedding through the diffusion process [10]. We provide more details on strokes initialization in Section 4.2.

As shown in Figure 4, in each step of the optimization, we feed the stroke parameters to a differentiable rasterizer \mathcal{R} to produce the raster sketch. We optimize over parameters θ such that $\mathcal{R} = \mathcal{S}(\theta)$ is close to a sample from the frozen latent diffusion model [30]. To perform this optimization, we use an input augmentation version of the SDS (ASDS) loss function, where plausible images have low loss and implausible images have a high loss. This results in the raster sketch always being coherent with the text prompt. The resulting sketch, as well as the sample from the frozen latent diffusion model, then defines a joint semantic and perceptual loss. We backpropagate the loss through the differentiable rasterizer \mathcal{R} and update the control points and opacity of strokes directly at each step until convergence of the loss function.

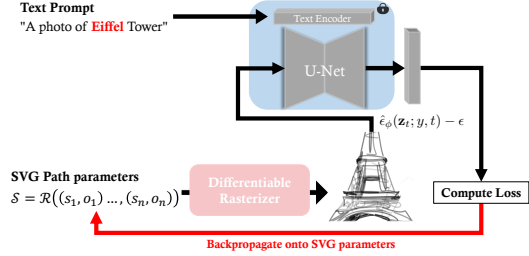


Figure 3: Pipeline overview. DiffSketcher accepts a set of control points and text prompts as input to generate a hand-drawn sketch.

4.1 Synthesis Through Optimization

We define a sketch as a set of n strokes $\{s_1, \dots, s_n\}$ with the opacity attribute placed on a white background. To represent each stroke, we use a two-dimensional Bézier curve with four control points $s_i = \{p_i^j\}_{j=1}^4 = \{(x_i, y_i)^j\}_{j=1}^4$ and one opacity attribute o_i . We incorporate the opacity of the strokes into the optimization process and use DiffSketcher semantics understanding to achieve a human-like *heavy and light sketch style*. The parameters of the strokes are fed to a differentiable rasterizer \mathcal{R} , which forms the raster sketch $\mathcal{S} = \mathcal{R}((s_1, o_1) \dots, (s_n, o_n)) = \mathcal{R}(\{\{p_1^j\}_{j=1}^4, o_1\}, \dots, \{\{p_n^j\}_{j=1}^4, o_n\})$. For simplicity, we define the parameter in \mathcal{R} as θ .

4.1.1 Vanilla Version: Fidelity to Generated Image

We start with a two-stage pipeline: First, we sample an image from the latent diffusion model [30] using a text prompt. Next, we optimize the control points to obtain a sketch that is consistent with the text prompt. To preserve the fidelity of the generated sample, we incorporate a **Joint Visual Semantic and Perceptual (JVSP)** loss to optimize the similarity of the synthesized sketches and the instance sampled from the frozen latent diffusion model [30]. We leverage the VAE [6] decoder \mathcal{D} to get the RGB pixel representation of $\hat{\mathcal{S}}_\phi(\mathbf{z}_t|y; t)$. Then, we jointly use the LPIPS [46] and CLIP visual encoders [27, 44] as depth structural similarity and visual semantic similarity metrics, respectively. Specifically, we use the following loss function:

$$\mathcal{L}_{\text{JVSP}} = \mathcal{L}_{\text{LPIPS}}(\mathcal{D}(\hat{\mathcal{S}}_\phi(\mathbf{z}_t|y; t)), \mathcal{R}(\theta)) + \sum_l \left\| \text{CLIP}_l(\mathcal{D}(\hat{\mathcal{S}}_\phi(\mathbf{z}_t|y; t))) - \text{CLIP}_l(\mathcal{R}(\theta)) \right\| \quad (4)$$

The $\mathcal{L}_{\text{JVSP}}$ loss function encourages the synthesized sketch to match the underlying semantics and perceptual details of the image sampled from LDM, leading to more realistic and visually appealing results. While vectorizing a rasterized diffusion sample is lossy, an input **Augmentation** version of the **SDS** (ASDS) loss can either finetune the results or optimize random control points from scratch to sample a sketch that is consistent with the text prompt. In the Sec 4.1.2, we introduce the ASDS loss to match the text prompt.

4.1.2 Augmentation SDS Loss: Fidelity to Text Prompt

To synthesize a vector sketch that matches a given text prompt, we directly optimize the parameters θ of the differentiable rasterizer \mathcal{R} that produces the raster sketch \mathcal{S} . We propose an input augmentation version of the SDS loss function to perform this optimization, which encourages plausible images to have low loss and implausible images to have a high loss. Given a raster sketch $\tilde{\mathcal{S}} \in \mathbb{R}^{H \times W \times 3}$, we combine *RandomPerspective*, *RandomResizedCrop* and *RandomAdjustSharpness* to get a data augmentation version of $\tilde{\mathcal{S}}_a \in \mathbb{R}^{512 \times 512 \times 3}$. Then, the LDM uses a VAE encoder [6] to encode $\tilde{\mathcal{S}}_a$ into a latent representation $\mathbf{z} = \mathcal{E}(\tilde{\mathcal{S}}_a)$, where $\mathbf{z} \in \mathbb{R}^{(H/f) \times (W/f) \times 4}$ and f is the encoder downsample factor. Then, we use the following ASDS loss function:

$$\nabla_\theta \mathcal{L}_{\text{ASDS}}(\phi, \mathcal{S} = \mathcal{R}(\theta)) \triangleq \mathbb{E}_{t, \epsilon, a} \left[w(t) (\hat{\epsilon}_\phi(\mathbf{z}_t; y, t) - \epsilon) \frac{\partial \mathbf{z}}{\partial \tilde{\mathcal{S}}_a} \frac{\partial \tilde{\mathcal{S}}_a}{\partial \theta} \right] \quad (5)$$

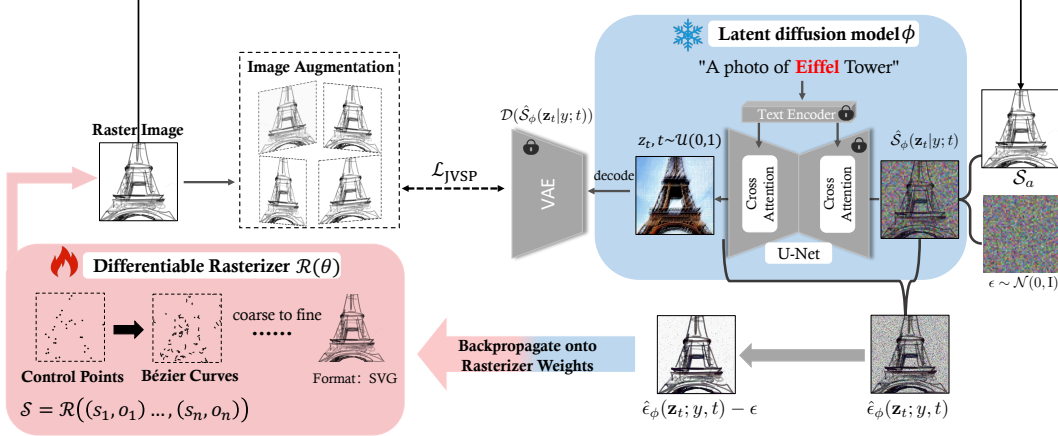


Figure 4: Optimization overview. To synthesize a sketch that matches the given text prompt, we optimize the parameters of the differentiable rasterizer \mathcal{R} that produces the raster sketch \mathcal{S} , such that the resulting sketch is close to a sample from the frozen latent diffusion model (the blue part of the picture). Since the diffusion model directly predicts the update direction, we do not need to backpropagate through the diffusion model; the model simply acts like an efficient, frozen critic that predicts image-space edits.

Where the weighting function $w(t)$ is a hyper-parameter. And we sample $t \sim \mathcal{U}(0.05, 0.95)$, avoiding very high and low noise levels due to numerical instabilities. Like DreamFusion [24], we set $\omega = 100$ for classifier-free guidance and higher guidance weights give improved sample quality. Intuitively, this loss perturbs \hat{S}_a with a random amount of noise corresponding to the timestep t , and estimates an update direction that follows the score function of the diffusion model to move to a higher density region. The ASDS loss function encourages the synthesized sketch to match the given text prompt, while also preserving the style and structure of the original sketch. At each iteration, we backpropagate the loss through the differentiable rasterizer and update the control points and opacity of strokes directly until convergence of the loss function.

Loss objectives of our final model. To further enhance the quality of the synthesized sketches, we incorporate the JVSP and ASDS losses. Specifically, we first obtain the initial results with the JVSP loss, then we fine-tune the differentiable rasterizer together with the SDS loss. We found such design can achieve the best performance. The ASDS loss predicts the gradient update direction directly, thus its loss value does not require weight balancing. In the JVSP loss, we set the weight of the LPIPS item to 0.2, and the weight of the CLIP visual item to 1. To compute the L2 distance between intermediate level activations of CLIP, we follow the CLIPasso [43] method and use layers 3 and 4 of the ResNet101 CLIP model. As shown in Figure 8, we compare the performance of the vanilla version with that of the version using only the ASDS loss, and the proposed final version. Our experiments show that the final version improves both the generation quality and efficiency.

4.2 Joint Attention-based Stroke Initialization

The highly non-convex nature of the ASDS loss function makes the optimization process susceptible to initialization, especially in multi-instance scenarios where strokes must be carefully placed to emphasize the overall semantics conveyed by free-hand sketching. We improve the convergence towards semantic depictions by initializing the curve control points based on the attention map of the text prompt conditional latent diffusion model. The UNet in the LDM has two types of attention mechanisms (the blue part), self-attention and cross-attention, as shown in Figure 5 where the yellow part represents the cross-attention visualization result, and the green part represents the self-attention visualization result. The structure and appearance of the image generated by the LDM [30] depend on the interaction between the pixels to the text embedding through the diffusion process [10], which is manifested in the cross-attention layer [42]. The visualization results indicate that the cross-attention layers control the relationship between the spatial layout of the image and each word in the prompt, while the self-attention layer affects the spatial layout and geometric structure of the generated image. With this observation, we linearly combine the probability distributions of the two attention maps to initialize the curve control points. Specifically, we pick a map in the cross-attention maps based on a text token and combine it with the averaged self-attention map. This process is formalized as

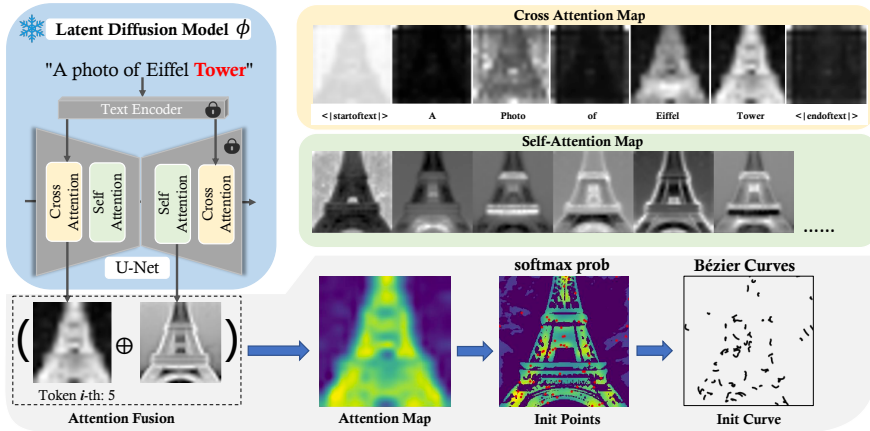


Figure 5: Strokes Initialization. The blue part of the figure represents the UNet in the LDM, which has two types of attention mechanisms: self-attention and cross-attention. The yellow and green parts respectively depict the visualization results of the cross-attention and self-attention. The gray part shows how the initial strokes are generated using a fused attention map. The dashed box represents the attention fusion, which is composed of the mean of the self-attention map and the cross-attention map corresponding to the 5-th text prompt token (“Tower”). We start at 1-th token, because 0-th token is taken up by the CLIP starting token.

FinalAttn = $\lambda * \text{CrossAttn}_i + (1 - \lambda) * \text{Mean}(\text{SelfAttn})$, where λ is the control coefficient and i indicates the i -th token in the text prompt. Finally, we normalize the fused attention map using softmax and use it as a distribution map to sample n positions for the first control point p_i^1 of each Bézier curve. The other three control points (p_i^2, p_i^3, p_i^4) are sampled within a small radius (0.05 of image size) around p_i^1 to define the initial set of Bézier curves $\{\{p_i^j\}_{j=1}^4\}_{i=1}^n$. Empirical results show that our attentional fusion-based initialization contributes significantly to the quality and rendering speed of the final sketch in comparison to the random initialization.

5 Results

	LDM's Result	Canny	CLIPasso	Ours
“Sailboat sailing in the sea on a clear day, realistic photo, professional photography”				
		Aesthetic : 4.3327 Top Predictions: correct : 87.7% ship : 10.1% vessel : 1.3%	Aesthetic : 4.1243 Top Predictions: correct : 80.9% ship : 14.8% vessel : 2.1%	Aesthetic : 5.00213 Top Predictions: correct : 91.6% ship : 6.7% vessel : 0.4%
“Analog photo of realistic lighthouse on island, night, focused, photo from distance”				
		Aesthetic : 4.5861 Top Predictions: correct : 98.3% observatory : 0.7% mountain : 0.3%	Aesthetic : 3.3128 Top Predictions: ship : 27.6% horse : 9.7% snake : 9.1%	Aesthetic : 4.2762 Top Predictions: correct : 92.7% sailboat : 2.8% inn : 1.1%
“Portrait of two white bunnies, super realistic, highly detailed”				
		Aesthetic : 4.2071 Top Predictions: correct : 98.9% dog : 0.4% mug : 0.2%	Aesthetic : 3.7280 Top Predictions: correct : 33.3% inn : 27.1% horse : 5.7%	Aesthetic : 4.9222 Top Predictions: correct : 96.9% apple : 1.0% inn : 0.6%
“Photorealistic painting of a fruit basket with fruit”				
		Aesthetic : 5.2122 Top Predictions: correct : 99.8% apple : 0.1% cat : 0.01%	Aesthetic : 4.1354 Top Predictions: correct : 47.0% mug : 14.1% vessel : 13.3%	Aesthetic : 6.3245 Top Predictions: correct : 99.6% apple : 0.1% vessel : 0.1%
“Real photo of sydney opera house”				
		Aesthetic : 3.4230 Top Predictions: correct : 99.9% sailboat : 0.02% inn : 0.01%	Aesthetic : 2.1973 Top Predictions: correct : 22.74% inn : 15.9% needle : 9.4%	Aesthetic : 4.3317 Top Predictions: correct : 99.4% needle : 0.1% sailboat : 0.1%

Figure 6: Comparison with Existing Methods.

5.1 Qualitative Evaluation

As shown in Figure 2, we demonstrate that our approach offers the ability to produce object-level and scene-level sketches based on a textual prompt, with the flexibility to manipulate the level of abstraction through stroke count. It is effective in generating accurate sketches regardless of prompt complexity, including simple or non-existent objects, iconic constructions, and detailed scenes. And the utilization of the robust prior of stable diffusion allows for a favorable initialization, promoting the production of high-quality sketches with significantly fewer iterations.

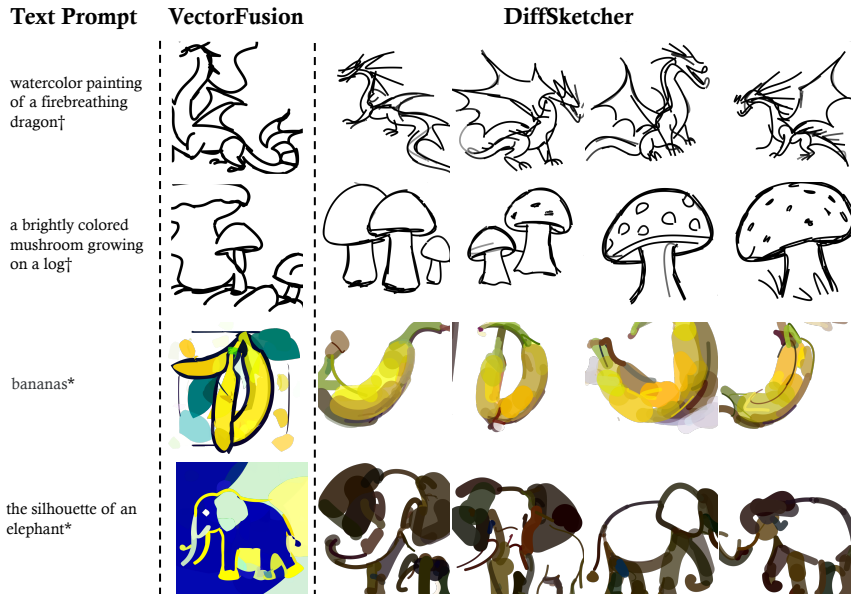


Figure 7: Qualitative comparison with VectorFusion(VF) [13]. VF’s results were copied from Figure 2 of its original paper, with a text prompt suffix of “minimal 2D line drawing trending on ArtStation”. In contrast, our results were optimized from scratch using ASDS without specifically designed text prompt suffix.

5.2 Comparison with Existing Methods

Figure 6 qualitatively compared our DiffSketcher with those of other CLIP-based [44] and edge extraction-based methods [2]. The Canny edge extraction algorithm extracts an excessive number of edges and produces untidy sketches, as observed in the first example in Figure 6. CLIPasso uses visual distance metrics to guide gradient-based optimization. On the task of drawing scene-level sketches, CLIPasso can only draw part of the foreground, and the background part is missing. DiffSketcher produces much cleaner vector sketches than baselines because we incorporate a generative prior of image appearance.

5.3 Quantitative Evaluation

Evaluating text-to-sketch synthesis is challenging due to the absence of ground truth sketches. Therefore, we focus on three indicators: consistency between the generated sketch and text prompt, the aesthetic quality of the sketch, and the recognition accuracy of the sketch. To measure the consistency between the generated sketch and input text, we calculate the mean of cosine similarity of CLIP embeddings for the generated sketches and the text captions used to generate them. Our method achieves a cosine similarity of 0.3494, which is higher than the 0.328 achieved by the Canny algorithm and the 0.3075 achieved by CLIPasso. Aesthetic appeal is subjective, and beauty is a personal experience and preference. However, the beauty of a hand-drawn sketch can be described in terms of various factors, such as line quality, texture, material, composition, style, and expressiveness. As an evaluation of our proposed method, we use CLIP-based aesthetic indicators [33] to calculate the aesthetic value for samples of multiple categories. Figure 6 shows the aesthetic value of various methods in some examples. Our method achieves a mean value of 4.8206 for the aesthetic value on a large number of examples, which is higher than the 4.3682 achieved by the Canny algorithm and the 4.0821 achieved by CLIPasso [44].

5.4 Ablation Study

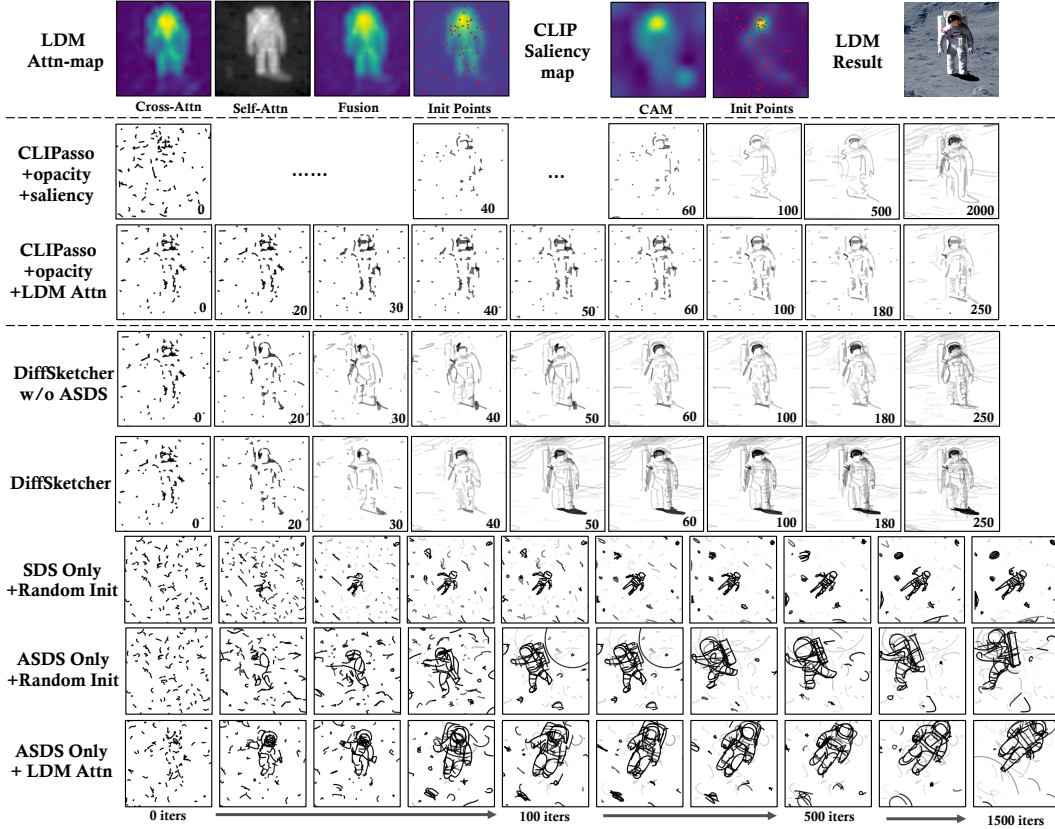


Figure 8: Qualitative results of ablation study. **Top**: two initialization strategies used by DiffSketcher (i.e., LDM Attention) and CLIPasso [44] (i.e., CAM [35] Saliency map). A result of sampling from LDM . The **2nd** and **3rd** rows: effect comparison of the two initialization strategies on the rate of convergence. The **4th** and **5th** rows: The effect of JVSP (Section 4.1.1) and ASDS loss (Section 4.1.2). The **5th** row shows the loss of SDS without data augmentation. The **6th** and **7th** rows: ASDS loss can lead to more diversity when used with random initialization. Text prompts in the figure: “Astronaut on Asteroid, galaxy background”

We conducted ablation studies to demonstrate the advantages of the proposed initialization strategy and to compare the effects of ASDS loss and JVSP loss. Fig 8 Top rows show two initialization strategies used by DiffSketcher, namely LDM Attention and CLIPasso [44], which are CAM [35] Saliency map. The attention level of the text-driven diffusion model outperforms CLIP, which is only identified based on the maximum difference perspective due to LDM’s superior generative ability. The cross-attention feature of LDM can efficiently activate relevant regions based on token areas, while the self-attention layer can effectively differentiate foreground from background down to the pixel level. By combining both mechanisms, the initialization area becomes more precise, allowing the renderer to place more initial points within the active region corresponding to the foreground object. As shown in Fig 8 2nd and 3rd. this results in a superior quality sketch with fewer optimization steps required. The proposed initialization strategy improves sampling quality and efficiency, which is critical for non-convex objective function optimization. The use of ASDS loss can guide the rendering process to produce morphic sketches when random initial points are used. However, without any semantic information, the resulting sketches may lack precision. In contrast, when initial points are informed by semantic knowledge, the ASDS optimization gains direction and stability, ultimately producing more refined sketches. Moreover, the integration of ASDS losses accelerates the model convergence process while enhancing the level of detail in the final sketch.

In DiffSketcher, our JVSP loss incorporates both CLIP loss and LPIPS loss, and it is important to note that ASDS and JVSP do not conflict with each other. As depicted in Fig. 8 of the manuscript,

the 4th and 6th rows highlight the effects of JVSP loss and ASDS loss, respectively. When only JVSP loss is used (4th row), the generated sample closely approximates the result of LDM. On the other hand, when only ASDS loss is employed (6th row), the generated sample aligns with the text prompt semantically, but does not follow the attention map of the LDM. Additionally, using ASDS loss results in more diverse sampling outcomes during the synthesis process. For instance, the location of the astronaut’s head may change throughout the drawing process when ASDS loss is used, while it remains in the same location when the JVSP loss is employed.

Considering these observations, we can summarize the features of JVSP loss and ASDS loss as follows: (1) JVSP loss: It constrains the alignment between the generated sketch and the LDM’s result, making it suitable for a two-stage pipeline. JVSP loss relies on the LDM’s result and allows modification through adjustments to the text prompt, providing control over the generated sketch. (2) ASDS loss: It does not rely on the LDM’s result and can be used for one-stage optimization. ASDS loss offers more flexibility, resulting in diverse generated samples.

In our full model, we leverage the advantages of both JVSP loss and ASDS loss by employing them for optimization. As demonstrated in the 5th row of our results (labeled “DiffSketcher”), when these two losses are combined, the synthesized sketches exhibit more intricate details and appear visually more realistic.

6 Conclusion

In this work, we have proposed a novel and effective approach to bridge the gap between natural language and free-hand sketches. By leveraging the power of pretrained text-to-image diffusion models, we have developed a method that can generate diverse and high-quality vector sketches based on textual input, without the need for large-scale datasets of sketches or sketch-text pairs. We have also explored different aspects of the model design, such as the stroke initialization strategies, choice of loss functions, and properties of strokes in the differentiable rasterizer, which provide valuable insights for future research. With further research and development, our proposed model, DiffSketcher, has the potential to be a valuable tool in various domains, such as design and education.

References

- [1] Ankan Kumar Bhunia, Salman Khan, Hisham Cholakkal, Rao Muhammad Anwer, Fahad Shahbaz Khan, Jorma Laaksonen, and Michael Felsberg. Doodleformer: Creative sketch drawing with transformers. In *Proceedings of the European conference on computer vision (ECCV)*, pages 338–355, 2022.
- [2] John Canny. A computational approach to edge detection. *IEEE Transactions on Pattern Analysis and Machine Intelligence*, PAMI-8(6):679–698, 1986.
- [3] Caroline Chan, Frédo Durand, and Phillip Isola. Learning to generate line drawings that convey geometry and semantics. In *Proceedings of the IEEE/CVF Conference on Computer Vision and Pattern Recognition (CVPR)*, pages 7915–7925, June 2022.
- [4] Shu-Yu Chen, Wanchao Su, Lin Gao, Shihong Xia, and Hongbo Fu. Deepfacedrawing: Deep generation of face images from sketches. In *ACM Transactions on Graphics (TOG)*, volume 39, pages 72–1. ACM New York, NY, USA, 2020.
- [5] Prafulla Dhariwal and Alexander Nichol. Diffusion models beat gans on image synthesis. In *Advances in Neural Information Processing Systems (NIPS)*, volume 34, pages 8780–8794, 2021.
- [6] Patrick Esser, Robin Rombach, and Bjorn Ommer. Taming transformers for high-resolution image synthesis. In *Proceedings of the IEEE/CVF conference on computer vision and pattern recognition (NIPS)*, pages 12873–12883, 2021.
- [7] Kevin Frans, Lisa Soros, and Olaf Witkowski. CLIPDraw: Exploring text-to-drawing synthesis through language-image encoders. In Alice H. Oh, Alekh Agarwal, Danielle Belgrave, and Kyunghyun Cho, editors, *Advances in Neural Information Processing Systems (NIPS)*, 2022.
- [8] Songwei Ge, Vedanuj Goswami, Larry Zitnick, and Devi Parikh. Creative sketch generation. In *International Conference on Learning Representations (ICLR)*, 2021.
- [9] David Ha and Douglas Eck. A neural representation of sketch drawings. In *International Conference on Learning Representations (ICLR)*, 2018.
- [10] Amir Hertz, Ron Mokady, Jay Tenenbaum, Kfir Aberman, Yael Pritch, and Daniel Cohen-or. Prompt-to-prompt image editing with cross-attention control. In *The Eleventh International Conference on Learning Representations (ICLR)*, 2023.
- [11] Jonathan Ho, Ajay Jain, and Pieter Abbeel. Denoising diffusion probabilistic models. In *Advances in Neural Information Processing Systems (NIPS)*, volume 33, pages 6840–6851, 2020.
- [12] Jonathan Ho and Tim Salimans. Classifier-free diffusion guidance. *arXiv preprint arXiv:2207.12598*, 2022.
- [13] Ajay Jain, Amber Xie, and Pieter Abbeel. Vectorfusion: Text-to-svg by abstracting pixel-based diffusion models. In *Proceedings of the IEEE/CVF Conference on Computer Vision and Pattern Recognition (CVPR)*, 2023.
- [14] Dmytro Kotovenko, Matthias Wright, Arthur Heimbrecht, and Bjorn Ommer. Rethinking style transfer: From pixels to parameterized brushstrokes. In *Proceedings of the IEEE/CVF Conference on Computer Vision and Pattern Recognition (CVPR)*, pages 12196–12205, 2021.
- [15] Mengtian Li, Zhe Lin, Radomir Mech, Ersin Yumer, and Deva Ramanan. Photo-sketching: Inferring contour drawings from images. In *2019 IEEE Winter Conference on Applications of Computer Vision (WACV)*, pages 1403–1412. IEEE, 2019.
- [16] Tzu-Mao Li, Michal Lukáč, Gharbi Michaël, and Jonathan Ragan-Kelley. Differentiable vector graphics rasterization for editing and learning. *ACM Trans. Graph. (Proc. SIGGRAPH Asia)*, 39(6):193:1–193:15, 2020.
- [17] Yi Li, Yi-Zhe Song, Timothy M Hospedales, and Shaogang Gong. Free-hand sketch synthesis with deformable stroke models. *International Journal of Computer Vision*, 122:169–190, 2017.

- [18] Runtao Liu, Qian Yu, and Stella X Yu. Unsupervised sketch to photo synthesis. In *Computer Vision—ECCV 2020: 16th European Conference, Glasgow, UK, August 23–28, 2020, Proceedings, Part III 16*, pages 36–52. Springer, 2020.
- [19] Xu Ma, Yuqian Zhou, Xingqian Xu, Bin Sun, Valerii Filev, Nikita Orlov, Yun Fu, and Humphrey Shi. Towards layer-wise image vectorization. In *Proceedings of the IEEE/CVF Conference on Computer Vision and Pattern Recognition (CVPR)*, pages 16314–16323, 2022.
- [20] Ben Mildenhall, Pratul P Srinivasan, Matthew Tancik, Jonathan T Barron, Ravi Ramamoorthi, and Ren Ng. Nerf: Representing scenes as neural radiance fields for view synthesis. *Communications of the ACM*, 65(1):99–106, 2021.
- [21] Piotr Mirowski, Dylan Banarse, Mateusz Malinowski, Simon Osindero, and Chrisantha Fernando. Clip-clop: Clip-guided collage and photomontage. *arXiv preprint arXiv:2205.03146*, 2022.
- [22] Alexander Mordvintsev, Nicola Pezzotti, Ludwig Schubert, and Chris Olah. Differentiable image parameterizations. *Distill*, 2018. <https://distill.pub/2018/differentiable-parameterizations>.
- [23] Alexander Quinn Nichol, Prafulla Dhariwal, Aditya Ramesh, Pranav Shyam, Pamela Mishkin, Bob McGrew, Ilya Sutskever, and Mark Chen. GLIDE: Towards photorealistic image generation and editing with text-guided diffusion models. In *Proceedings of the 39th International Conference on Machine Learning (ICML)*, volume 162 of *Proceedings of Machine Learning Research*, pages 16784–16804, 17–23 Jul 2022.
- [24] Ben Poole, Ajay Jain, Jonathan T. Barron, and Ben Mildenhall. Dreamfusion: Text-to-3d using 2d diffusion. In *The Eleventh International Conference on Learning Representations (ICLR)*, 2023.
- [25] Thomas Porter and Tom Duff. Compositing digital images. In *Proceedings of Conference on Computer Graphics and Interactive Techniques, SIGGRAPH '84*, page 253–259, 1984.
- [26] Yonggang Qi, Guoyao Su, Pinaki Nath Chowdhury, Mingkang Li, and Yi-Zhe Song. Sketchlattice: Latticed representation for sketch manipulation. *2021 IEEE/CVF International Conference on Computer Vision (ICCV)*, pages 933–941, 2021.
- [27] Alec Radford, Jong Wook Kim, Chris Hallacy, Aditya Ramesh, Gabriel Goh, Sandhini Agarwal, Girish Sastry, Amanda Askell, Pamela Mishkin, Jack Clark, et al. Learning transferable visual models from natural language supervision. In *International conference on machine learning*, pages 8748–8763. PMLR, 2021.
- [28] Aditya Ramesh, Prafulla Dhariwal, Alex Nichol, Casey Chu, and Mark Chen. Hierarchical text-conditional image generation with clip latents. *arXiv preprint arXiv:2204.06125*, 2022.
- [29] Pradyumna Reddy, Michael Gharbi, Michal Lukac, and Niloy J Mitra. Im2vec: Synthesizing vector graphics without vector supervision. In *Proceedings of the IEEE/CVF Conference on Computer Vision and Pattern Recognition (CVPR)*, pages 7342–7351, 2021.
- [30] Robin Rombach, Andreas Blattmann, Dominik Lorenz, Patrick Esser, and Björn Ommer. High-resolution image synthesis with latent diffusion models. In *Proceedings of the IEEE/CVF Conference on Computer Vision and Pattern Recognition (CVPR)*, pages 10684–10695, 2022.
- [31] Chitwan Saharia, William Chan, Saurabh Saxena, Lala Li, Jay Whang, Emily L Denton, Kamyar Ghasemipour, Raphael Gontijo Lopes, Burcu Karagol Ayan, Tim Salimans, et al. Photorealistic text-to-image diffusion models with deep language understanding. In *Advances in Neural Information Processing Systems (NIPS)*, volume 35, pages 36479–36494, 2022.
- [32] Peter Schaldenbrand, Zhixuan Liu, and Jean Oh. Styleclipdraw: Coupling content and style in text-to-drawing synthesis. *arXiv preprint arXiv:2111.03133*, 2021.
- [33] Christoph Schuhmann. Improved aesthetic predictor. <https://github.com/christophschuhmann/improved-aesthetic-predictor>, 2022.

- [34] Christoph Schuhmann, Romain Beaumont, Richard Vencu, Cade Gordon, Ross Wightman, Mehdi Cherti, Theo Coombes, Aarush Katta, Clayton Mullis, Mitchell Wortsman, et al. Laion-5b: An open large-scale dataset for training next generation image-text models. *arXiv preprint arXiv:2210.08402*, 2022.
- [35] Ramprasaath R Selvaraju, Michael Cogswell, Abhishek Das, Ramakrishna Vedantam, Devi Parikh, and Dhruv Batra. Grad-cam: Visual explanations from deep networks via gradient-based localization. In *Proceedings of the IEEE international conference on computer vision (ICCV)*, pages 618–626, 2017.
- [36] I-Chao Shen and Bing-Yu Chen. Clipgen: A deep generative model for clipart vectorization and synthesis. *IEEE Transactions on Visualization and Computer Graphics*, 28(12):4211–4224, 2021.
- [37] Jascha Sohl-Dickstein, Eric Weiss, Niru Maheswaranathan, and Surya Ganguli. Deep unsupervised learning using nonequilibrium thermodynamics. In *Proceedings of the International Conference on Machine Learning (ICML)*, volume 37, pages 2256–2265, 2015.
- [38] Yang Song and Stefano Ermon. Generative modeling by estimating gradients of the data distribution. In *Advances in Neural Information Processing Systems (NIPS)*, volume 32, 2019.
- [39] Yang Song, Jascha Sohl-Dickstein, Diederik P Kingma, Abhishek Kumar, Stefano Ermon, and Ben Poole. Score-based generative modeling through stochastic differential equations. In *International Conference on Learning Representations (ICLR)*, 2021.
- [40] Yingtao Tian and David Ha. Modern evolution strategies for creativity: Fitting concrete images and abstract concepts. In *Artificial Intelligence in Music, Sound, Art and Design*, pages 275–291. Springer, 2022.
- [41] Zhengyan Tong, Xuanhong Chen, Bingbing Ni, and Xiaohang Wang. Sketch generation with drawing process guided by vector flow and grayscale. In *Proceedings of the Conference on Artificial Intelligence (AAAI)*, volume 35, pages 609–616, 2021.
- [42] Ashish Vaswani, Noam Shazeer, Niki Parmar, Jakob Uszkoreit, Llion Jones, Aidan N Gomez, Łukasz Kaiser, and Illia Polosukhin. Attention is all you need. *Advances in neural information processing systems (NIPS)*, 30, 2017.
- [43] Yael Vinker, Yuval Alaluf, Daniel Cohen-Or, and Ariel Shamir. Clipascene: Scene sketching with different types and levels of abstraction. *arXiv preprint arXiv:2211.17256*, 2022.
- [44] Yael Vinker, Ehsan Pajouheshgar, Jessica Y Bo, Roman Christian Bachmann, Amit Haim Bermano, Daniel Cohen-Or, Amir Zamir, and Ariel Shamir. Clipasso: Semantically-aware object sketching. *ACM Transactions on Graphics (TOG)*, 41(4):1–11, 2022.
- [45] Saining Xie and Zhuowen Tu. Holistically-nested edge detection. In *Proceedings of the IEEE International Conference on Computer Vision (ICCV)*, pages 1395–1403, 2015.
- [46] Richard Zhang, Phillip Isola, Alexei A Efros, Eli Shechtman, and Oliver Wang. The unreasonable effectiveness of deep features as a perceptual metric. In *IEEE/CVF Conference on Computer Vision and Pattern Recognition (CVPR)*, 2018.